Nanoscale Advances

ROYAL SOCIETY OF CHEMISTRY

PAPER

View Article Online
View Journal | View Issue

Cite this: *Nanoscale Adv.*, 2020, **2**, 2497

Chemical affinity and dispersibility of boron nitride nanotubes†

C. S. Torres Castillo, C. Bruel and J. R. Tavares *

Received 18th February 2020
Accepted 4th May 2020

DOI: 10.1039/d0na00136h

rsc.li/nanoscale-advances

Boron nitride nanotubes (BNNTs) are electrically insulating nanoparticles that display highly competitive elastic modulus and thermal conductivity. Long presented as potential fillers for nanocomposite applications, their poor dispersibility in most commodity polymers has, however, limited their spread. In this work, the chemical affinity of purified BNNTs, measured in terms of Hansen solubility parameters (HSP), were obtained through sedimentation tests in a wide set of organic solvents, taking into account relative sedimentation time. The parameters obtained were $\{\delta_d; \delta_p; \delta_h\} = \{16.8; 10.7; 14.7\} \pm \{0.3; 0.9; 0.3\}$ $MPa^{1/2}$, with a Hildebrand parameter, $\delta_t = 24.7$ $MPa^{1/2}$ and a sphere radius of 5.4 $MPa^{1/2}$. The solubility parameters were determined considering complete dispersion of the purified nanomaterial, as well as the viscosity and density of the host solvent. These factors, combined with the high purity of the BNNTs, are crucial to minimize the uncertainty of the HSP characterization. Such refined values provide necessary insights both to optimize the solvent casting of unmodified BNNTs, and to orient the surface modification efforts that would be needed to integrate these nanomaterials into a wider range of host matrices.

Introduction

Boron nitride nanotubes are counterparts to carbon nanotubes (CNTs) in which C atoms are replaced by alternating B and N atoms in a honeycomb network (Fig. 1).[1–4] First synthesized in 1995,[3] these nanomaterials have properties that may outmatch those of CNTs for high temperature or electrical insulation related applications. Compared with CNTs, BNNTs display a competitive Young modulus (~1.18 TPa) and thermal conductivity (up to ~350 W m K^{-1}). Contrary to CNTs, they have a high thermal stability (up to 1100 °C in air)[4] and are electrical insulators, with a constant band gap of ~5.5 eV. CNTs degrade from ~500 °C in air and are conductive or semi-conductive materials.[1,3] The two nanotube types also differ in their physical appearance: pure BNNTs present a white color while CNTs are black.[3]

The partially ionic B–N bonds in BNNTs bring about their unique properties.[3,4] A difference in electronegativity between B and N atoms leads to the formation of local dipole moments, providing BNNTs with a polar behavior.[3]

BNNTs find potential applications as a reinforcing agents in polymeric and ceramic materials[4] and, due to their high surface area, are good candidates for hydrogen storage devices.[3,5] In addition, because of their unique combination of thermal conductivity and electrical insulation, BNNTs can be used for heat dissipation in electronics and computers.[6–8] However, in spite of these attractive properties, their incorporation into composites has been hindered mainly by production limitations: few methods exist to produce large quantities and high-quality material (high crystallinity, small diameter and few walls).[2,3] In 2013, the National Research Council of Canada patented an industrially-scalable approach for the increased production (20 g h^{-1}) of few-walled and small diameter (~5 nm) BNNTs.[9–11] In brief, hexagonal boron nitride (h-BN), N_2 and H_2 are used as precursors in a thermal plasma reactor. These are dissociated into individual atoms (B, N and H) and recombine as BNNTs. Hydrogen acts as a catalyst and is crucial in reaching a high production rate for BNNTs. It enables the formation of nitrogen reactive species and impedes the formation of N_2 as a side product.[9] While high production rates have therefore become possible, there remains little available knowledge to reliably disperse BNNTs in solvents and polymers.

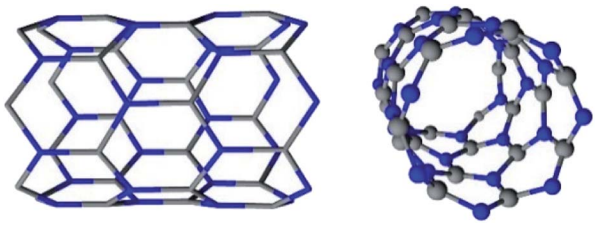

Fig. 1 Structure of single-walled BNNTs. Boron atoms are in blue, nitrogen atoms in grey.

CREPEC, Chemical Engineering Department, Polytechnique Montréal, 2900 Edouard Montpetit Blvd, Montréal, Québec, QC H3T 1J4, Canada. E-mail: jason.tavares@polymtl.ca

† Electronic supplementary information (ESI) available. See DOI: 10.1039/d0na00136h

As a starting point to predict dispersion behaviour, Mutz *et al.*[12] determined the Hildebrand solubility parameter of BNNTs, on the basis of the Hildebrand–Scatchard solution theory. Using this parameter, they proposed a list of potential good solvents for dispersing these nanotubes. However, predicting chemical affinity by considering only the Hildebrand solubility parameter (δ_t) is not reliable, unless the chemical in question displays a purely non-polar behavior, such as saturated aliphatic hydrocarbons.[13] Otherwise, dispersive, polar, and hydrogen bonding interactions should be considered.

In another work, Tiano *et al.*[14] determined the Hansen solubility parameters (HSP) of few-walled BNNTs (up to three walls) through sedimentation tests. They used as-synthesized material without any further purification, containing boron nanoparticles as impurities. These impurities not only have different surface chemistry than the nanotubes but also different density (~2.3 *vs.* 1.4 g mL^{-1}), which significantly modifies the sedimentation rate. In addition, some discrepancies are found in their work regarding the determination of good solvents.

Solubility parameters of purified BNNTs are necessary to orient surface modification efforts. Indeed, according to the literature, several covalent[15–17] and non-covalent[18–22] functionalization methods have been carried out on BNNTs in attempts to properly disperse them in a specific medium. However, in most cases, the methodology applied is not specifically tailored or targeted, relying instead on general assumptions to promote dispersion. Given that surface modification approaches can be complicated and time consuming, that they employ costly molecules such as surfactant/modifier agents and that, in the case of covalent functionalization, the intrinsic properties of BNNTs are often modified (initial sp^2 structure altered), these efforts must be guided by a strong initial knowledge of the BNNTs dispersion to target the most appropriate surface treatment.

In order to have a proper characterization of the dispersibility of purified BNNTs, here, we apply the Hansen solubility theory, taking into account differences in density and viscosity of the solvents, to characterize the surface properties of BNNTs through sedimentation tests. Having defined their HSP, three scenarios may be addressed. First, surface modification may be performed depending on the chemical affinity (or lack of it) between the BNNTs and the polymeric matrix. Second, if the functionalization method is solvent-based, then, knowing the proper solvents to disperse BNNTs will allows us to select the best media in which to conduct surface modification. Third, when using solvents casting techniques, the selection of an appropriate solvent will improve nanocomposite fabrication.

Theory

Solubility parameters rely on the principle that "like seeks like", which states that liquids with similar parameters will form homogeneous mixtures.[13] Transposed to particles, this principle means that solvents will better disperse particles with similar surface chemistry. The Hansen solubility method has been successfully used to characterize solid surfaces such as pigments,[23] fibers, nanoparticles[14,24–31] and fillers.

Solubility parameters, also known as *cohesion parameters*, can be related to the amount of energy necessary to evaporate a liquid.[13] This is a measure of the total energy required to keep the molecules of a liquid together, expressed as the cohesive energy density (E/V) (eqn (1)):

$$\delta_t = (E/V)^{1/2} \quad (1)$$

where δ_t ($MPa^{1/2}$), V (mol cm^{-3}), and E (kJ mol^{-1}), are the Hildebrand solubility parameter, the molar volume of the solvent and its latent heat of evaporation, respectively.[13]

The Hildebrand solubility parameter can be divided in three components related to dispersion (δ_d), polar (δ_p) and hydrogen bonding (δ_h) interactions.[13] These are known as *Hansen solubility parameters* (HSP) (eqn (2)) and provide a measure of the strength of the interactions that a chemical may form in a specific solvent.[13]

$$\delta_t^2 = \delta_d^2 + \delta_p^2 + \delta_h^2 \quad (2)$$

Dispersion forces (δ_d), produced by atomic interactions, accounts for non-polar London interactions.[13] Polar forces (δ_p) are present when permanent dipole-permanent dipole interactions are formed. These interactions occur at the molecular level and the dipole moment is used to determine this type of attractions.[13] Like in polar forces, hydrogen bonding interactions (δ_h) take place at a molecular level. δ_h has been generally used to describe the capability of electron exchange determined by Lewis' acid and base theory.[23] δ_h has been divided into subparameters such as acid–base, dispersion, induction, orientation, as well as proton-donors and proton-acceptors. However, the use of a single parameter to describe hydrogen bonding interactions has been proven to give satisfactory results.[13]

Based on Hansen solubility theory, it is possible to plot the particle of interest and solvents in a three-dimensional (3D) space (Hansen space) with their corresponding HSP $\{\delta_d; \delta_p; \delta_h\}$ as coordinates. The center of the solubility sphere is determined by the particle coordinates with an experimental radius, R_o. The solvents with coordinates located inside the sphere will disperse the particle, with higher dispersibility for the solvents that are closer to the center of the sphere.[13] The distance between the solvent and the particle, R_a, in the Hansen space can be determined applying eqn (3):

$$R_a^2 = 4(\delta_{d1} - \delta_{d2})^2 + (\delta_{p1} - \delta_{p2})^2 + (\delta_{h1} - \delta_{h2})^2 \quad (3)$$

$$\mathrm{RED} = \frac{R_a}{R_o} \quad (4)$$

The ratio between R_a and R_o (eqn (4)), known as the relative energy difference (RED), estimates the position of the solvent in the solubility sphere.[13] RED < 1 indicates that the solvent will disperse the particle. For RED = 1, partial dispersion is expected and for RED > 1, the particle will not disperse in the solvent. HSP can also be used for binary mixtures of solvents (co-solvents).

When determining the HSP of nanoparticles, several factors should be considered, owing to different interactions that may occur. For instance, Bergin *et al.*[24] demonstrated that increasing the diameter of the nanotubes decreases δ_t by reducing the surface to volume ratio: this structural link between δ_t and morphology is also expected for BNNTs (eqn (5)).

$$\delta_t = 2\sqrt{\frac{E_{S,T}}{D}} \quad (5)$$

where $E_{S,T}$ and D correspond to the total nanotube surface energy and to the nanotube diameter, respectively. Exploring this in the context of CNTs, they demonstrated that the Hildebrand parameter decreases when D increases.[24]

Empirically, HSP may be determined by depositing small quantities of particles in test tubes containing a fixed volume of liquid and subsequently agitating.[13] Stability is assessed based on the presence of agglomerates in suspension, assessed visually or through spectroscopic means. If the particle size of the solid is large (>5 μm), surface effects are less significant compared to particles with smaller sizes (<0.01 μm). Nonetheless, viscosity and buoyancy effects can impede proper analysis of a solid suspension. To compensate for differences in density and viscosity, a relative sedimentation time (RST) can be used instead of absolute sedimentation time, t_{sed}, (eqn (6)).[13]

$$\mathrm{RST} = t_{sed}\left(\frac{\rho_p - \rho_s}{\eta}\right) \quad (6)$$

where ρ_p and ρ_s refer to the densities of particle and the solvent and η is the viscosity of the solvent. For the determination of solubility parameters, the HSPiP software is typically used.[32] A description of the mathematical analysis is presented in the ESI.†

Experimental part

Materials and methods

Purified BNNTs were provided by Tekna Plasma Systems, Inc. (Sherbrooke, Qc, Canada) in the form of buckypapers (2 cm × 2 cm). They were obtained from the previously described induction thermal plasma process.[9,33] The as-obtained BNNTs possessed a beige color, attributed to the presence of amorphous boron.[9,34] These impurities were removed through the purification method described by Cho *et al.*[34] Briefly, the as-obtained BNNTs were dried for 3 h at 150 °C. They were then pre-heated in a quartz tube at 105 °C in an Ar atmosphere, keeping the temperature constant for 20 min. The quartz tube was then filled with Cl_2. The temperature was raised to 750 °C, under a flow of 1 standard liter per min of Cl_2. The exposure time was set at 1 min per gram of as-obtained BNNTs. These selective chlorine etching conditions were used to remove boron allotropes, including $B_xN_yH_z$ derivatives.[34] The system was then purged with N_2 and allowed to cool under a steady flow of N_2. The purified material was subsequently bath sonicated in methanol. Despite the purification process, SEM images suggest that some BN hollow cages are, however, still present in the material.[9,34] These structures are also visible on our TEM images (Fig. 2C and D).

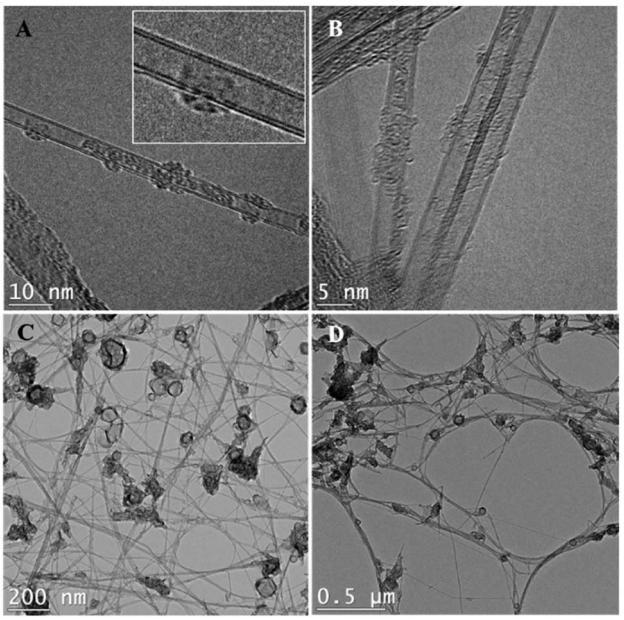

Fig. 2 Representative TEM images of BNNTs dispersed in ethanol. (A and B) BNNTs have a diameter of approximately 5 nm. The inset in (A) shows they are double walled. (C and D) BNNT length is on the order of a few μm, and some BN hollow cages remain in the material.

Organic solvents were obtained by chemical suppliers and were used without any further purification. Most of them were of high purity (≥99%) with exception of D-limonene (96%) and ethanol (95%). The list of solvents employed, as well as their physical properties (density, viscosity and molar volume) and HSP, are available in Tables 1 and S1.† Solvent selection considered the list of solvents proposed by Hansen for sedimentation tests, for which solubility parameters have been validated experimentally,[13] and expanded with a few additional solvents: ethyl benzoate, D-limonene and heptane, whose HSP values were determined through modelling.

Microscopy

TEM analysis was performed in BNNT dispersions using ethanol as a solvent. In brief, 1 mg of BNNTs was added to 10 mL of anhydrous ethanol and the resulting mixture was sonicated with a probe sonicator supplying 500 J of energy. A drop of the solution was deposited on a copper TEM grid and dried overnight. The analyses were performed using a Jeol JEM 2100F transmission electron microscope in bright field imaging mode, operating at 200 kV.

Sedimentation tests

10 mL of solvent were added to 1 mg of BNNTs in a glass vial of diameter 2.5 cm. This concentration was chosen as an intermediate value to form stable BNNTs dispersions in different solvents, according to previous works.[12,14]

To disperse the nanoparticles, a Cole–Parmer probe sonicator was employed with an operation frequency of 20 kHz using a cylindrical probe (type 410–08). The treatment consisted of pulsations operating with 5 s ON/2 s OFF cycles set at 30% of

Table 1 HSP, sedimentation time, dispersion state, R_a, and RED of the solvents used in sedimentation tests. Solvents are classified based on their dispersion states at the end of the sedimentation period (Fig. S4)

Solvent	δ_d (MPa$^{1/2}$)	δ_p (MPa$^{1/2}$)	δ_h (MPa$^{1/2}$)	Sedimentation time (h)	R_a	RED
Good dispersion state						
N,*N*′-Dimethylacetamide	16.8	11.5	10.2	48.0	5.36	1.00
N,*N*′-Dimethylformamide	17.4	13.7	11.3	42.6	4.69	0.88
Ethanol	15.8	8.8	19.4	51.3	5.45	1.00
2-Propanol	15.8	6.1	16.4	78.5	5.30	0.97
Intermediate dispersion state						
Acetone	15.5	10.4	7.0	14.1	8.13	1.51
Acetonitrile	15.3	18.0	6.1	14.0	11.7	2.16
Ethyl acetate	15.8	5.3	7.2	20.6	9.46	1.75
Ethyl benzoate	17.9	6.2	6.0	114	10.0	1.87
Methanol	15.1	12.3	22.3	23.8	8.83	1.62
Methyl ethyl ketone	16.0	9.0	5.1	15.8	9.88	1.83
Propylene carbonate	20.0	18.0	4.1	267	14.4	2.67
Tetrahydrofuran	16.8	5.7	8.0	25.8	8.36	1.55
Poor dispersion state						
Acetic acid	14.5	8.0	13.5	65.8	5.47	1.00
tert-Butanol	15.2	5.1	14.7	139	6.45	1.19
Chloroform	17.8	3.1	5.7	529	12.0	2.22
Cyclohexane	16.8	0	0.2	39.7	18.0	3.34
Dichloromethane	17.0	7.3	7.1	72.3	8.34	1.55
Dimethyl sulfoxide	18.4	16.4	10.2	142	7.94	1.48
1,4-Dioxane	17.5	1.8	9.0	81.4	10.7	1.98
Ethylene glycol[a]	17.0	11.0	26.0	1573	11.3	2.09
Formamide	17.2	26.2	19.0	255	16.1	2.98
Heptane	15.3	0	0	13.7	18.4	3.42
D-Limonene	17.2	1.8	4.3	38.9	13.7	2.54
Toluene	18.0	1.4	2.0	26.8	15.9	2.96
Additional solvents						
Benzyl alcohol[a,b]	18.4	6.3	13.7	342	5.53	1.02
Water[b]	15.1	20.4	16.5	50.6	10.4	1.93

[a] Reaching a good dispersion state required a stronger sonication. [b] Additional test solvent but not considered for the HSP analysis.

amplitude and a power in the range of 20–30 W. A total energy of 500 J mg_{BNNTs}^{-1} was used, which is high compared to typical standards for nanomaterial dispersion (*e.g.* 10 J mg^{-1} required to disperse cellulose nanocrystals in water),[35] attributable to the BNNTs high aspect ratio. To prevent any overheating, the vials were kept in an ice bath during sonication. The resulting suspensions were kept in a quiescent state at room temperature to allow the nanoparticles to sediment. The density of BNNTs was obtained from the literature[12,36] and an average of 1.5 g cm^{-3} was used. A relative sedimentation time (RST) of 1.03 $\times$ 10^{11} s^2 m^{-2} was considered, corresponding to an absolute sedimentation time (t_{sed}) of 48 h in *N*,*N*′-dimethylacetamide (DMAc). This solvent was chosen as a reference because it remained in a good dispersion state even after two days. The calculated absolute sedimentation time for each solvent is shown in Table 1.

Results and discussion

Ultrasonication and dispersion

According to TEM images (Fig. 2), the BNNTs used in the dispersions are doubled-walled (Fig. 2A and B) with a diameter of ~5 nm and a length of a few micrometers (Fig. 2C and D). These dimensions agree with the results reported by Kim *et al.*[9] where nanotubes with 2, 4 or 5 walls were obtained. The most common damages induced by ultrasonication treatments to BNNTs are peeling, shortening, and formation of Y-junctions or nanoribbons. All these phenomena are detectable through TEM,[37–40] namely for dispersion in ethanol, the solvent that was used in the preparation of the TEM grids, which has been reported to induce peeling under some circumstances.[37] However, based on our own images and on a comparison with those prior to sonication,[9] we have no reasons to believe that our ultrasonication conditions may cause significant damages to the BNNTs. The effect of a more severe ultrasonication, as performed in benzyl alcohol and ethylene glycol, was not investigated and we cannot rule out that some morphological damages occurred under these harsher conditions. That being said, the main driver for morphological changes, cavitation, is notoriously less efficient in viscous media.[41]

Pictures of the dispersions were taken immediately after sonication (Fig. S1†) and after their respective sedimentation time (Fig. S4†). According to Fig. S1,† nine solvents were able to

form good BNNT dispersions. These solvents were: ethanol (EtOH), propylene carbonate, 2-propanol (IPA), dimethyl acetamide (DMAc), dimethyl formamide (DMF), ethyl benzoate, dimethyl sulfoxide (DMSO), formamide and tetrahydrofuran (THF). All are Lewis bases, and are hence susceptible to interact with B atoms in the BN structure by sharing a pair of electrons. Over time, however, BNNTs progressively lost part or all their stability in propylene carbonate, ethyl benzoate, DMSO, formamide, and THF. This suggests that other phenomena may be at play besides Lewis acid–base interactions. Results presented in Table 1 report the dispersion observed at the end of the sedimentation time. At this point, only four solvents remain good: DMAc, DMF, EtOH, and IPA.

Dispersions in methanol (MeOH), methyl ethyl ketone (MEK), acetonitrile, acetone and ethyl acetate showed some dispersed particles at the top of the vial, while some sedimented at the bottom. On the other hand, when using ethylene glycol (EG), agglomerates of BNNTs were observed. The formation of these agglomerates most probably happened because the energy provided during sonication was not sufficient in such a highly viscous solvent (20.9 mPa s). In order to properly disperse the nanotubes, the dispersion was repeated, applying higher energy during sonication. An energy of 1800 J mg_{BNNTs}^{-1} was used. This new system is shown in Fig. S2† and, given its good dispersion behaviour after applying higher energy, EG has been added to the list of good media (thus bringing the total to 10 solvents).

In toluene, cyclohexane and heptane, BNNTs lost their stability and stuck to the glass right after sonication (Fig. S1†). These solvents are the three least polar and, in this case, our results align with those of Tiano *et al.*[14] for hexane. The instability of BNNTs can be attributed to a large difference in polarity between the nanotubes and the solvent. Due to a difference in electronegativity between B and N atoms, BN structures possess a dipolar moment.

This finding concurs with previous works on hexagonal boron nitride (h-BN) films, showing these are hydrophilic, with water contact angles of 50–55°.[42,43] However, there is controversy concerning the hydrophilicity of BNNTs films. Some studies have determined that BNNTs films are superhydrophobic, with contact angles in the range of 145–167°.[43–45] However, morphological characteristics in the films such as the packing density, length and alignment of the nanotubes[43] as well as the roughness and surface chemical heterogeneities[46] have an impact on the wettability of BNNTs films. In addition, theoretical studies have demonstrated that the spreading of a liquid over a highly curved surface is different from that on a flat surface,[42] with high surface curvature being associated with more hydrophobic behavior.[43]

Time-dependent dispersion state

In order to evaluate the evolution of the dispersions, three solvents were studied over a period of 150 h: propylene carbonate, ethyl benzoate and DMSO. These were chosen because, while their dispersion state was good immediately after sonication (Fig. S1†), it worsened over time (Fig. S3†). This emphasizes the need to determine a normalized sedimentation time in order to make objective evaluations of the dispersions.

The interval of time after which observation is performed varies due to differences in viscosity and density for each solvent. In order to compensate for these variations, a corrected relative sedimentation time (RST) (eqn (6)) is employed.[13] The calculated absolute sedimentation times, t_{sed}, for ethyl benzoate, DMSO and propylene carbonate were 114, 142 and 267 h, respectively. At 114 h, the dispersion state in ethyl benzoate showed a cloudy region at the top of the vial (around 20% of the volume) and the rest (80% of the volume) are swollen particles (Fig. S3B, S4A and B†). For DMSO, at 142 h after sonication, phase separation can be observed. In the case of propylene carbonate, the dispersion state observed at 267 h (Fig. S4A and B†) is similar to that observed at 150 h (Fig. S3A†). Given these observations at t_{sed}, these 3 solvents can no longer be considered "good" as they were for $t = 0$ observations in the previous section. It is worth noting that the cloudy agglomerates formed by BNNTs over time may be easily be redispersed by simply hand mixing the vials.

Dispersion end state

The quality of the dispersions was evaluated after their respective sedimentation time, t_{sed} (Table 1). The dispersions were classified as good, intermediate or poor (Fig. 3). Good solvents were able to form dispersions that were cloudy, but uniformly throughout the whole vial (Fig. 3A). Intermediate solvents presented dispersed material at the top of the vial while having sedimented BNNTs at the bottom (Fig. 3B). Poor solvents led to the formation of phase separation, with transparent regions at the top of the vial (Fig. 3C).

24 organic solvents were used for these sedimentation tests (Table 1). Dispersion in water was also conducted, but this solvent was not considered for the analysis because it has a strong tendency to structure itself in clusters, which may alter its HSP.[13] Four solvents were able to form cloudy and uniform dispersions of BNNTs (Fig. S4†): DMAc, DMF, ethanol and 2-propanol. These solvents contain amide or hydroxyl groups on their structure, which may lead to hydrogen bonding interactions with the nanotubes. In fact, these four are Lewis bases, characterized by the ability to donate a pair of electrons. On the

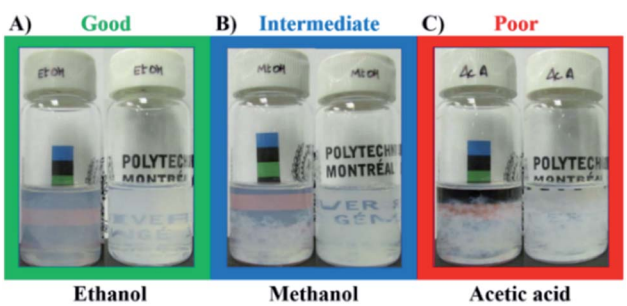

Fig. 3 Dispersibility of BNNTs at t_{sed} in (A) ethanol, (B) methanol, and (C) acetic acid.

other hand, B atoms on BN nanostructures present an electron deficiency, and thus, make them vulnerable to interactions with Lewis bases such as amines.[21,47] These interactions have in fact been specifically exploited by researchers aiming to non-covalently surface modify BNNTs. Xie *et al.*[20] used diamine-terminated polyethylene glycol (PEG) to functionalize the surface of BNNTs in order to disperse them in water. Similarly, Pal *et al.*[21] used trioctylamine and tributylamine to modify the BNNTs, while Maguer *et al.*[48] employed quinuclidine for modification, and Iannitto *et al.*[49] exploited similar chemistry in an ammonia plasma system.

As can be seen in Table 1, the calculated RED (eqn (4)) for these four good solvents was in the range of 0.88–1.0, which indicates that the solvents will be located inside or in the borders of the sphere. *N*,*N*′-Dimethylformamide and 2-propanol were found inside the sphere while *N*,*N*′-dimethylacetamide and ethanol were in the border.

Intermediate solvents were acetone, methanol, THF, ethyl acetate, acetonitrile, ethyl benzoate, MEK and propylene carbonate, with calculated RED values (eqn (4)) in the range of 1.51–2.67. These solvents possess δ_d and δ_p similar to the solvents classified as "good", but a significantly lower δ_h (Table 1). Low values of this parameter would prevent hydrogen bonding interactions required to obtain total dispersion of BNNTs. The exception to this was methanol, with an extremely high δ_h. For acid–base Lewis interactions to happen, a certain compatibility between the donor and acceptor is necessary. When the donor is much stronger than the acceptor, the former may prefer to interact with itself. In the case of methanol (the donor), it is likely that its molecules might have been able to self-associate, hiding most of their OH groups within itself and leaving the CH_3 groups exposed at the surface of the clusters.[32] The HSP of "clustered" methanol have been reported as $\{\delta_d; \delta_p; \delta_h\}_{Cluster} = \{14.7; 5; 10\}$ $MPa^{1/2}$,[32] where δ_d and δ_h are significantly lower compared to the standard HSP of methanol $\{\delta_d; \delta_p; \delta_h\}_{MeOH} = \{15.1; 12.3; 22.3\}$ $MPa^{1/2}$. Therefore, these CH_3 groups should not been able to interact with the BNNTs.

It is worth noting that different types of interparticle forces are expected during the assembly of nanoparticles. These include van der Waals forces, magnetic and electrostatic forces, repulsive steric, confining or jamming forces, solvation, structural and depletion forces, capillary forces, convective forces and friction and lubrication forces.[50] Their study would require a more detailed analysis, beyond the scope of the present work.

Dispersions with phase separation (*i.e.* "poor") at t_{sed} were observed in chloroform, acetic acid, DMSO, toluene, cyclohexane, heptane, D-limonene, formamide, 1,4-dioxane, ethylene glycol, *tert*-butanol and dichloromethane (DCM). The highest RED values (RED > 3) were obtained when non-polar solvents were used, reaching values of 3.34 and 3.42 for cyclohexane and heptane, respectively.

HSP analysis

Having probed the dispersibility of BNNTs in a large set of solvents, it becomes possible to determine their HSP using the HSPiP software. Solvents are classified as good (score = 1) or bad (score = 0) and their respective score ("0" or "1") is inputted into the HSPiP software. Calculations are performed based on the maximisation of a desirability function, FIT, that relies on the HSP distance, R_a.[32] FIT reaches a maximum of 1.0 when a sphere of center $\{\delta_d; \delta_p; \delta_h\}$ and of radius R_0 may be fitted to simultaneously include all the good solvents while excluding all the bad ones. When this is impossible, FIT is decreased by a factor that considers the various HSP distances. In circumstances where several combinations yield the same FIT, the software calculates an uncertainty on the true position of the sphere's center. Details and equations are provided in ESI and in Table S2.†

Since we witnessed three categories of behavior for the dispersions (good, intermediate, and poor), various combinations may be considered for the fitting. In the following paragraph, we will first attribute the grade 1 to good solvents only (DMF, DMAc, ethanol and 2-propanol), and grade 0 for intermediate and poor ones. Then, the grade 1 to good and intermediate solvents alike and grade 0 for poor solvents only. Two sets of HSP coordinates will thus be determined, corresponding to a main and to an extended chemical affinity, respectively.

Attributing the grade 1 to good solvents (green circles) only, the Hansen space for the BNNTs has them distributed inside the sphere, while the intermediate (blue triangles – grade 0) and poor solvents (red squares – grade 0) are located outside (Fig. 4). 2D plots (Fig. 5) help to visualize the data presented in Fig. 4. These provide upper and lower bounds for the various HSP. From Fig. 5A and B it can be concluded that the dispersive component (δ_d) of the BNNTs is in the range of 15.8–17.4 $MPa^{1/2}$. From Fig. 5A and C, the polar component (δ_p) should be in the interval of 6.1–13.7 $MPa^{1/2}$.

The hydrogen-bonding component (δ_h) can be determined from Fig. 5B and C, in the range of 10.2–19.4 $MPa^{1/2}$. The

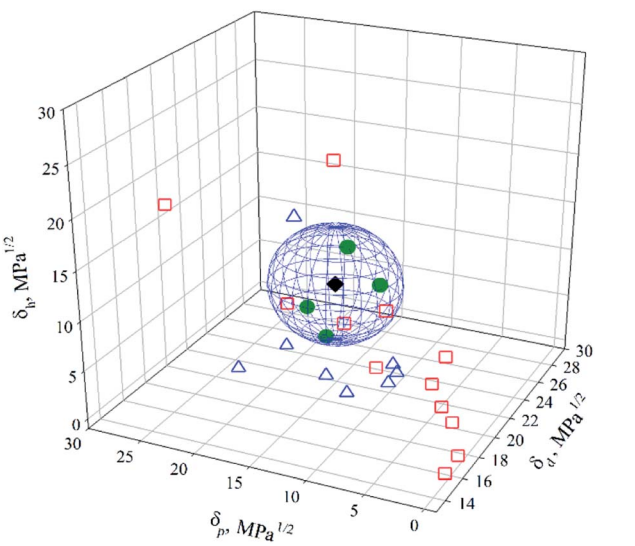

Fig. 4 Hansen space of BNNTs. The green circles correspond to the good solvents, the blue triangles to intermediate ones and the red squares to poor ones. The black diamond represents the centre of the sphere. Full symbols correspond to solvents inside the sphere while empty symbols to solvents outside.

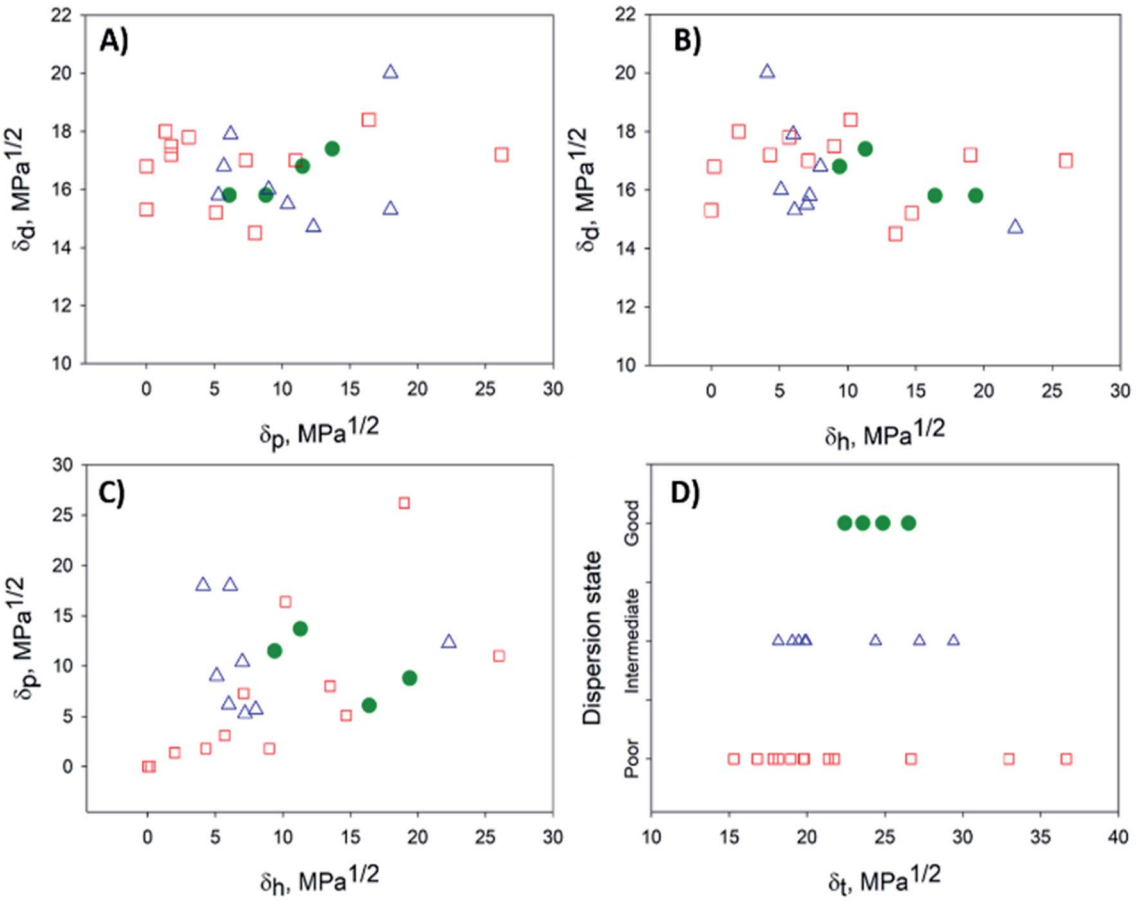

Fig. 5 2D projections to help with the visualization of the data presented in Fig. 4. (A) δ_d *vs.* δ_p, (B) δ_d *vs.* δ_h, (C) δ_p *vs.* δ_h and (D) dispersion state *vs.* δ_t. Good, intermediate and bad solvents are represented by green, blue and red circles, respectively.

dispersion state *versus* the Hildebrand parameter (δ_t) is plotted in Fig. 5D. Good solvents for the dispersion of BNNTs will be those with a δ_t in the range of 22.4–26.5 $MPa^{1/2}$, that also respect conditions for R_a (eqn (3)) and RED (eqn (4)) such that RED < 1. However, as mentioned before, the selection of potential solvents should be done based on the HSP distance (eqn (3)) considering the three HSP: dispersive, polar and hydrogen bonding interactions, not just the Hildebrand parameter.

The first set of calculated HSP for BNNTs is: $\{\delta_d; \delta_p; \delta_h\}_{main} = \{16.8; 10.7; 14.7\} \pm \{0.3; 0.9; 0.3\}$ $MPa^{1/2}$. The radius of the sphere is $R_0 = 5.4$ $MPa^{1/2}$ and the $\delta_t = 24.7$ $MPa^{1/2}$. A FIT = 1.0 was obtained, meaning that all the grade 1-solvents were located inside the sphere and all the grade 0-solvents outside. The HSP of BNNTs obtained in this work differ from those obtained by Tiano *et al.*[14] In their work, the center of the sphere was determined by $\{\delta_d; \delta_p; \delta_h\}_{Tiano} = \{16.8; 10.7; 9.0\}$ $MPa^{1/2}$ with a $\delta_t = 21.8$ $MPa^{1/2}$ and $R_0 = 4.3$ $MPa^{1/2}$. They used as-synthesized material containing boron nanoparticles as impurities, affecting not only the surface chemistry of the nanotubes but also their density. They determined 4 good solvents: DMAc, DMF, acetone and *N*-methyl-2-pyrrolidone (NMP). However, based on their vial pictures, the dispersion in acetone should not be qualified as "good", as a large fraction of nanotubes are sedimented after settling for 1 week. This behaviour is corroborated in our experiments, where just after sonication some nanotubes sedimented while other fractions were suspended (Fig. S1†). In addition, when comparing the HSP of acetone $\{\delta_d; \delta_p; \delta_h\}_{ACE} = \{15.5; 10.4; 7\}$ $MPa^{1/2}$ with the intervals proposed in the present work to estimate good solvents for BNNTs, only the δ_d value is within its corresponding interval and a RED = 1.51 (eqn (4)) was obtained. This indicates that acetone is not a good solvent to disperse the BNNTs. Regarding NMP, with $\{\delta_d; \delta_p; \delta_h\}_{NMP} = \{18; 12.3; 7.2\}$ $MPa^{1/2}$, similar to acetone, only δ_p is within the interval proposed, while δ_d and δ_h are outside the range provided. The calculated RED = 1.49 (eqn (4)) indicates that NMP is situated outside the sphere, and thus considered as a poor solvent. In both cases, a low value of δ_h prevents some hydrogen bonding interactions from happening, impeding complete dispersion of BNNTs.

An explanation for the deviations between Tiano's results[14] and those presented in this work could be the concentration (0.25 mg mL^{-1}, compared with 0.1 mg mL^{-1} in this work). This could have caused some dispersions to oversaturate and thus, favored a sedimentation of the BNNTs. Another factor arises from the sedimentation time: their analysis considered an absolute sedimentation time of 1 week for all the dispersions. As discussed earlier, the use of a normalized sedimentation time, t_{sed}, is preferred. Variations in chemical composition, as

well as in length and diameter of the nanotubes could also affect the HSP determination.[14,24] Tiano et *al.*[14] concluded that their HSP correlate well with the BNNTs used. However, they stated that dispersions should be repeated if different methods of synthesis and/or purification processes are used, this being the main limitation of their work.

In the present study, we minimized the uncertainty in the HSP values by using purified material and compensating for differences in density and viscosity of the solvents. Nonetheless, the uncertainty of $\pm\{0.3; 0.9; 0.3\}$ $MPa^{1/2}$ with which the HSP of BNNTs were determined means that the border of the sphere is a soft one. With an HSP radius of $R_0 = 5.4$ $MPa^{1/2}$, it translates in an uncertainty of roughly ± 0.2 on RED values: any predictions made on solvents whose RED is comprised between 0.8 and 1.2 must be considered with caution. This may be highlighted by investigating the behaviour of BNNTs in a solvent like benzyl alcohol. With HSP of $\{\delta_d; \delta_p; \delta_h\}_{BA} = \{18.4; 6.3; 13.7\}$ $MPa^{1/2}$, benzyl alcohol has a RED value (eqn (4)) of ~1.02, meaning that it is located right at the outer edge of the border of the BNNTs' Hansen sphere. With a RED strictly above 1, it should thus be a poor solvent. However, it is right in the middle of the uncertain area for RED values. Experimentally, it was found to be a good solvent (Fig. S4†). This proves the soft nature of the border between good and poor solvents when RED values are close to 1. Calculating the RED according to Tiano's results yields a value of 1.33, which suggests that their range of uncertainty regarding RED values was probably even larger than ours. It is worth noting that, because of its high viscosity (5.47 mPa s), a higher energy (1600 J mg_{BNNTs}^{-1}) was applied during sonication to properly disperse the BNNTs in benzyl alcohol. Our analysis is performed based on the assumption that the BNNTs were not damaged by this more intense ultrasonication step.

To make a graphical comparison between the Hansen space obtained by Tiano *et al.*[14] and the one obtained in this work, a 3D graph containing both spheres was plotted (Fig. 6). The blue sphere corresponds to the results obtained in this work, $\{\delta_d; \delta_p; \delta_h\}_{main} = \{16.8; 10.7; 14.7\}$ $MPa^{1/2}$, while the black one to Tiano's, $\{\delta_d; \delta_p; \delta_h\}_{Tiano} = \{16.8; 10.7; 9.0\}$ $MPa^{1/2}$. Even though δ_d and δ_p are the same in both cases, the differences in δ_h and R_0 cause the spheres to locate in different regions. A partial overlap is observed in the space limited by $\delta_d = 15.8$–17.8 $MPa^{1/2}$, $\delta_p = 7.3$–13.7 $MPa^{1/2}$ and $\delta_h = 9.4$–14.7 $MPa^{1/2}$. These HSP values are within the intervals proposed in this work for the prediction of good solvents for BNNTs. The center of the intersection region was found at $\{\delta_d; \delta_p; \delta_h\}_{intersection} = \{16.8; 10.6; 11.5\}$ $MPa^{1/2}$. Only two solvents were found in that space: DMF, located within the overlapped region, and DMAc, located in the border. On the other hand, 2-propanol was found inside the blue sphere, centered at $\{\delta_d; \delta_p; \delta_h\}_{main}$, while ethanol and benzyl alcohol were on the border. DCM and acetone were located inside the black sphere, with center at $\{\delta_d; \delta_p; \delta_h\}_{Tiano}$. Three of the four expected solvents (DMF, DMAc and acetone) were located inside this sphere. The fourth one, NMP, with coordinates $\{\delta_d; \delta_p; \delta_h\}_{NMP} = \{18; 12.3; 7.2\}$ $MPa^{1/2}$, was not used as a test solvent in the present work. Instead, DCM, with $\{\delta_d; \delta_p; \delta_h\}_{DCM} = \{17; 7.3; 7.1\}$ $MPa^{1/2}$, was found to be inside the black sphere. Although

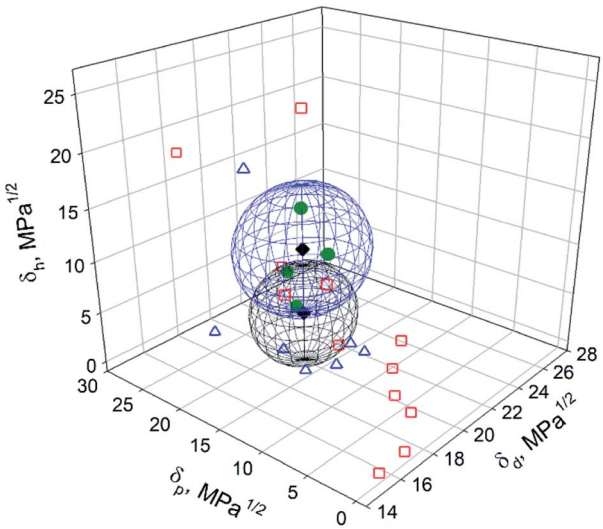

Fig. 6 Hansen space of BNNTs obtained in this work (blue sphere) and the results obtained by Tiano *et al.*[14] (black sphere). The green circles, blue triangles and red squares correspond to good, intermediate and poor solvents determined in this work.

δ_d and δ_h possess similar values, a difference of 5 $MPa^{1/2}$ is observed in the polar component, δ_p. According to Tiano's results, the dispersion in DCM was not good and a phase separation was observed 30 min after sonication, with swollen particles at the bottom of the vial. These results are in agreement with the ones obtained in the present work.

To visualize the influence of partial dispersibility in the Hansen space, a second analysis was performed, expanding the list of good solvents with the intermediate ones (Table 1). These solvents were acetone, methanol, THF, ethyl acetate, acetonitrile, ethyl benzoate, MEK and propylene carbonate. They were scored as "1" and added to the list of good solvents previously defined (DMAc, DMF, EtOH and IPA). The "poor" solvents were kept scored "0". The resulting Hansen sphere (gray sphere) is shown in Fig. 7. The Hansen space determined previously, considering total dispersibility of BNNTs (blue sphere) and the one obtained by Tiano *et al.*[14] (black sphere) are also plotted. As can be seen in Fig. 7, the blue and black spheres are located inside the gray one. This trend was expected because good solvents should remain suitable when good and intermediate solvents are considered.[13] However, the addition of more solvents to the list of "good" ones will modify the coordinates and radius of the Hansen sphere. In this case, the solvents added to the list of good ones possess a wide range of HSP, covering different spaces in the Hansen space but leaving some uncovered regions.

The Hansen solubility parameters of the gray sphere were $\{18.8; 13.9; 14.4\}_{extended} \pm \{0.2; 0.4; 0.3\}$ $MPa^{1/2}$, with a radius $R_0 = 11.4$ $MPa^{1/2}$. A FIT = 0.434 was obtained, meaning that some good solvents were located outside the sphere while some poor ones are inside (see ESI†). DCM, acetic acid, DMSO and *tert*-butanol, considered as bad solvents (Table 1), were located inside this gray Hansen sphere while methanol, MEK, acetonitrile, ethyl benzoate and ethyl acetate (good solvents) are located

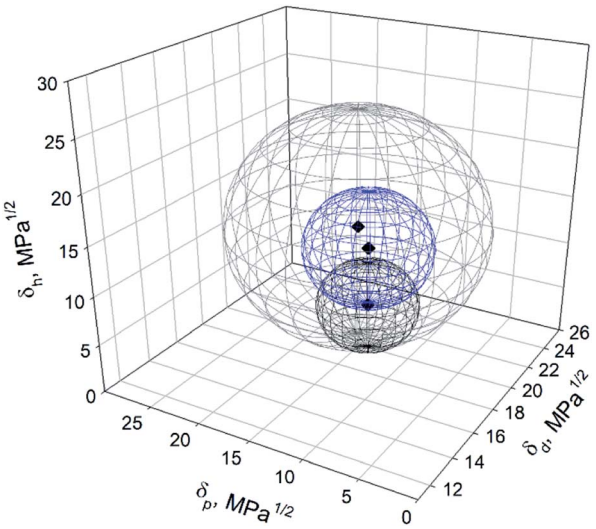

Fig. 7 Hansen space of BNNTs obtained in this work considering total dispersibility (blue sphere), partial dispersibility (gray sphere) and Tiano's results (black sphere).

outside. This relocation of the solvents by the HSPiP software could have happened due to the large differences in their HSP, making difficult to get a good FIT. Low values in the *desirability function* FIT will provide less reliable values of the HSP of the particle in question.

As mentioned earlier, Mutz *et al.*[12] determined the total solubility parameter, $\delta_t = 18.53$ MPa$^{1/2}$, using static light scattering and the Flory and Hildebrand–Scatchard solution theories. The BNNTs used had a diameter in the range of 30–100 nm, in comparison with the 5 nm diameter nanotubes used in our work. Based on the expression developed by Bergin *et al.*[24] for CNTs (eqn (5)), larger nanotubes have lower δ_t values. We suggest it may be the reason why our δ_t is higher than the one reported by Mutz et *al*.[12] Based on that, Mutz et *al*. proposed a list of *potential* good solvents: ethyl acetate, isophorone, diamyl phthalate, vinyltoluene and *cis*-1,2-dichloroethyelene. However, as mentioned before, the prediction of solvents considering only the Hildebrand solubility parameter (δ_t) is not reliable for particles presenting polar and hydrogen interactions.[13] In addition, it is pertinent to note that one of the good solvents predicted was ethyl acetate, which is indeed able to partially disperse the BNNTs, as demonstrated in this work (intermediate score).

Conclusions

In this work, the Hansen solubility parameters of purified BNNTs were determined for the first time through sedimentation tests accounting for relative sedimentation time. The HSP obtained were $\{\delta_d; \delta_p; \delta_h\} = \{16.8; 10.7; 14.7\} \pm \{0.3; 0.9; 0.3\}$ MPa$^{1/2}$. The radius of the sphere was $R_0 = 5.4$ MPa$^{1/2}$ and the Hildebrand parameter $\delta_t = 24.7$ MPa$^{1/2}$. Evaluation of the dispersion state in different organic solvents was done after an appropriate relative sedimentation time, taking into account differences in density and viscosity of the solvents. However, the method of synthesis used, the presence of impurities and the diameter of the nanotubes play an important role when determining their HSP. Four solvents were able to form uniform dispersions of BNNTs. These were DMF, DMAc, ethanol and 2-propanol. It is thought that the hydrogen bonding interactions between the solvents and the nanotubes are crucial for good dispersion. Having defined the HSP of BNNTs more precisely, this data can now be used to guide dispersion into host matrices, as well as methodologies for surface treatment.

Conflicts of interest

There are no conflicts to declare.

Acknowledgements

The authors would like to acknowledge the Natural Sciences and Engineering Research Council of Canada (NSERC), Prima Québec, the Mexican National Council for Science and Technology (CONACyT), Tekna Plasma Systems, Michelin Canada and Polytechnique Montréal. The Fonds de Recherche du Québec - Nature et Technologies (FRQNT) provided C. Bruel with a scholarship (number 208324). Mr Paul-Henri Verger and Ms Alekhya V. Veerubhotla are also thanked for their valuable contributions to the early versions of this work.

Notes and references

1 C. Zhi, Y. Bando, C. C. Tang, Q. Huang and D. Golberg, *J. Mater. Chem.*, 2008, **18**, 3900.
2 M. Terrones, J. M. Romo-Herrera, E. Cruz-Silva, F. López-Urías, E. Muñoz-Sandoval, J. J. Velázquez-Salazar, H. Terrones, Y. Bando and D. Golberg, *Mater. Today*, 2007, **10**, 30.
3 C. Zhi, Y. Bando, C. Tang and D. Golberg, *Mater. Sci. Eng., R*, 2010, **70**, 92.
4 J. Wang, C. H. Lee and Y. K. Yap, *Nanoscale*, 2010, **2**, 2028.
5 T. Terao, Y. Bando, M. Mitome, K. Kurashim, C. Y. Zhi, C. C. Tang and D. Golberg, *Phys. E*, 2007, **40**, 2551.
6 J. Su, Y. Xiao and M. Ren, *Phys. Status Solidi A*, 2013, **12**, 2699.
7 C. Zhi, Y. Bando, T. Terao, C. Tang, H. Kuwahara and D. Golberg, *Adv. Funct. Mater.*, 2009, **19**, 1857.
8 X. Huang, C. Zhi, P. Jiang, D. Golberg, Y. Bando and T. Tanaka, *Adv. Funct. Mater.*, 2013, **23**, 1824.
9 K. Kim, C. T. Kingston, A. Hrdina, M. B. Jakubinek, J. Guan, M. Plunkett and B. Simard, *ACS Nano*, 2014, **8**, 6211.
10 K. Kim, M. B. Jakubinek, Y. Martinez-Rubi, B. Ashrafi, J. Guan, K. O'Neill, M. Plunkett, A. Hrdina, S. Lin, S. Denommee, C. Kingston and B. Simard, *RSC Adv.*, 2015, **5**, 41186.
11 K. S. Kim, C. Kingston and B. Simard, Patent app. no. US61/813324, 2013.
12 M. Mutz, E. Eastwood and M. Dadmun, *J. Phys. Chem. C*, 2013, **117**, 13230.
13 C. M. Hansen, *Hansen solubility parameters: A user's handbook*, Taylor & Francis, 2nd edn, 2007.

14 A. L. Tiano, L. Gibbons, M. Tsui, S. I. Applin, R. Silva, C. Park and C. C. Fay, *Nanoscale*, 2016, **8**, 4348.
15 C. Zhi, Y. Bando, C. Tang, S. Honda, K. Sato, H. Kuwahara and D. Golberg, *Angew. Chem.*, 2005, **44**, 7932.
16 C. Zhi, Y. Bando, T. Terao, C. C. Tang, H. Kuwahara and D. Golberg, *Chem.–Asian J.*, 2009, **4**, 1536.
17 S. Zhou, C. Y. Ma, Y. Y. Meng, H. F. Su, Z. Zhu, S. L. Deng and S. Y. Xie, *Nanotechnology*, 2012, **23**, 055708.
18 J. Yu, Y. Chen and B. M. Cheng, *Solid State Commun.*, 2009, **149**, 763.
19 C. Lee, D. Zhang and Y. K. Yap, *J. Phys. Chem. C*, 2011, **116**, 1798.
20 S. Xie, W. Wang, K. A. Shiral Fernando, X. Wang, Y. Lin and Y. P. Sun, *Chem. Commun.*, 2005, 3670.
21 S. Pal, S. R. C. Vivekchand, A. Govindaraj and N. R. Rao, *J. Mater. Chem.*, 2007, **17**, 450.
22 Z. Gao, C. Zhi, Y. Bando, D. Golberg and T. Serizawa, *Appl. Mater. Interfaces*, 2011, **3**, 627.
23 S. Süß, T. Sobisch, W. Peukert, D. Lerche and D. Segets, *Adv. Powder Technol.*, 2018, **29**, 1550.
24 S. D. Bergin, Z. Sun, D. Rickard, P. V. Streich, J. P. Hamilton and J. N. Coleman, *ACS Nano*, 2009, **3**, 2340.
25 H. T. Ham, Y. S. Choi and I. J. Chung, *J. Colloid Interface Sci.*, 2005, **286**, 216.
26 S. Detriche, G. Zorzini, J. F. Colomer, A. Fonseca and J. B. Nagy, *J. Nanosci. Nanotechnol.*, 2008, **8**, 6082.
27 S. Detriche, J. B. Nagy, Z. Mekhalif and J. Delhalle, *J. Nanosci. Nanotechnol.*, 2009, **9**, 6015.
28 Y. Hernandez, M. Lotya, D. Rickard, S. D. Bergin and J. N. Coleman, *Langmuir*, 2010, **26**, 3208.
29 S. Gårdebjer, M. Andersson, J. Engström, P. Restorp, M. Persson and A. Larsson, *Polym. Chem.*, 2016, **7**, 1756.
30 C. Bruel, J. Tavares, P. Carreau and M. Heuzey, *Carbohydr. Polym.*, 2019, **205**, 184.
31 C. Bruel, T. S. Davies, P. J. Carreau, J. R. Tavares and M.-C. Heuzey, *J. Colloid Interface Sci.*, 2020, **574**, 399.
32 S. Abbott, C. M. Hansen and H. Yamamoto, *Hansen solubility parameters in practice*, 2008.
33 K. Kim, M. Couillard, H. Shin, M. Plunkett, D. Ruth, C. Kingston and B. Simard, *ACS Nano*, 2018, **12**, 884.
34 H. Cho, S. Walker, M. Plunkett, D. Ruth, R. Iannitto, Y. Martinez-Rubi, K. S. Kim, C. M. Homenick, A. Brinkmann, M. Couillard, S. Dénommée, J. Guan, M. B. Jakubinek, Z. J. Jakubek, C. T. Kingston and B. Simard, *Chem. Mater.*, 2020, DOI: 10.1021/acs.chemmater.0c00144.
35 Q. Beuguel, J. Tavares, P. Carreau and M. C. Heuzey, *J. Colloid Interface Sci.*, 2018, **516**, 23.
36 C. Zhi, Y. Bando, C. Tang and D. Golberg, *Solid State Commun.*, 2011, **151**, 183.
37 D. Kim, S. Nakajima, T. Sawada, M. Iwasaki, S. Kawauchi, C. Zhi, Y. Bando, D. Golberg and T. Serizawa, *Chem. Commun.*, 2015, **51**, 7104.
38 Y. Lin, T. V. Williams, T.-B. Xu, W. Cao, H. E. Elsayed-Ali and J. W. Connell, *J. Phys. Chem. C*, 2011, **115**, 2679.
39 C. Zhi, Y. Bando, C. Tang, H. Kuwahara and D. Golberg, *Adv. Mater.*, 2009, **21**, 2889.
40 Q. Huang, Y. Bando, C. Zhi, D. Golberg, K. Kurashima, F. Xu and L. Gao, *Angew. Chem.*, 2006, **45**, 2044.
41 J. A. Gallego-Juarez, and K. F. Graff, *Power Ultrasonics Applications of High-intensity Ultrasound*, Woodhead Publishing, Cambridge, U.K., 2014.
42 C. Lee, J. Drelich and Y. K. Yap, *Langmuir*, 2009, **25**, 4853.
43 L. Boinovich, A. M. Emelyanenko, A. S. Pashinin, C. H. Lee, J. Drelich and Y. K. Yap, *Langmuir*, 2012, **28**, 1206.
44 L. Li, H. L. Li, S. Ramakrishnan, X. J. Dai, K. Nicholas, Y. Chen, Z. Chen and X. Liu, *J. Phys. Chem. C*, 2012, **116**, 18334.
45 C. Lee, Boron Nitride Nanotubes: Synthesis, Characterization, Ph.D. dissertation, Functionalization and Potential Applications, 2010.
46 C. Bruel, S. Queffeulou, T. Darlow, N. Virgilio and J. R. Tavares, *Can. J. Chem. Eng.*, 2019, **97**, 832.
47 Y. Liao, Z. Chen, J. W. Connell, C. C. Fay, C. Park, J. W. Kim and Y. Lin, *Adv. Funct. Mater.*, 2014, **24**, 4497.
48 A. Maguer, E. Leroy, L. Bresson, E. Doris, A. Loiseau and C. Mioskowski, *J. Mater. Chem.*, 2009, **19**, 1271.
49 R. Iannitto, H. Shin, Y. Martinez-Rubi, B. Simard and S. Coulombe, *ACS Appl. Nano Mater.*, 2020, **3**(1), 294–302.
50 Y. Min, M. Akbulut, K. Kristiansen, Y. Golan and J. Israelachvili, *Nat. Mater.*, 2008, **7**, 527.

